analytical chemistry

pubs.acs.org/ac Article

A Multi-Channel System for Temperature Sensing of Neural Stem Cells in Adherent Culture

Jiaxu Ding, Jing Li, Fang Yang,* and Ning Gu*

Cite This: *Anal. Chem.* 2020, 92, 3270−3275 Read Online

ACCESS | Metrics & More | Article Recommendations | Supporting Information

ABSTRACT: Neural stem cells (NSCs) can gradually proliferate or differentiate during adherent culture. It is found that stem cells have different temperature characteristics in different physiological states. In order to detect the temperature of NSCs during adherent culture, in this study, we have designed a temperature monitoring system, in which a thin-film platinum resistor was used as the sensor. The NSCs were seeded on the sensor, and the data acquisition device was connected to the host computer via Bluetooth. Results indicate that there are about 5000 cells attached on the surface of each sensor, and the cell viability is maintained at about 90% after 24 h culture. An electrostatic force microscope (EFM) result proves that there is no electric field on the sensor surface to influence the activity of NSCs. This system can work continuously for more than 24 h with 0.05 °C detection sensitivity. Furthermore, the significant temperature change of NSCs is observed when stimulated by different concentrations of thyroid hormone, which demonstrates that the temperature change related to cell activity. Therefore, by detecting the temperature of the cell population, the fabricated system can provide reference information for studying the metabolic state of NSCs, as well as physiological responses of cells under various conditions in biomedical applications.

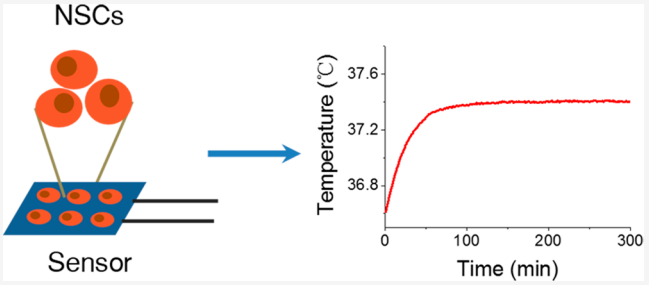

Neural stem cells are a subtype of progenitor cells in the nervous system that can self-renew and generate both neurons and glia. It has gained increasing interest over the past decades because of the broad potential for regenerative medical applications.[1−3] Its proliferation and differentiation characteristics have broad application prospects in promoting the repair of damaged central nervous system. Although NSCs have been cultured in in vitro culture media for cell transplantation therapy or to obtain neurotrophic factor,[4,5] the mechanism of proliferation and differentiation of NSCs during in vitro culture is still unclear.[6−9]

Metabolic control is another important regulator of stem cell activity. Stem cells seem to be in a metabolic state that is different from their progeny.[10,11] Normally, the mature cells rely on mitochondrial oxidative phosphorylation as the primary source of adenosine-triphosphate (ATP) generation. Instead, NSCs largely depend on glycolytic energy production.[12−14] Studies have shown that the external temperature can regulate the growth and development of cells.[15,16] Therefore, it is necessary to develop temperature detection methods at the thousand-cell level, which enables a more comprehensive analysis of stem cell behavior.

In recent years, many methods have been developed to detect cell temperature. (1) The thermocouple probe based on the Seebeck effect: it is capable of converting a temperature signal into an electromotive force signal, thereby detecting the temperature change of a single cell with high precision.[17,18] (2) Luminescence-based thermometry: the living cells are labeled with a material such as fluorescent protein. The changes in the temperature of the living cells are reflected by changes in characteristics such as the wavelength, intensity, and lifetime of the fluorescent signal.[19−21] (3) Atomic force microscope (AFM)-based scanning thermal probe: a temperature sensor at the top of the scanning probe is applied to image the surface temperature of the object at the nanometer level.[22,23]

Although the above-mentioned methods are capable of detecting the temperature of cells, they all have their own limitations. For example, thermocouples can only detect the temperature of a single cell and need to be inserted into the interior of the cell when applied measurement. It is a lossy measurement. Luminescence-based thermometers require suitable materials and need to be improved in terms of repeatability and stability. Scanning thermal probes are rarely used for real-time measurement of cell temperature due to the complexity of the operation.[24]

In order to overcome these limitations, herein, a multi-channel temperature measurement system based on thin-film platinum resistor was developed. As shown in Figure 1, the

Received: November 11, 2019
Accepted: January 27, 2020
Published: February 5, 2020

https://dx.doi.org/10.1021/acs.analchem.9b05134
Anal. Chem. 2020, 92, 3270−3275

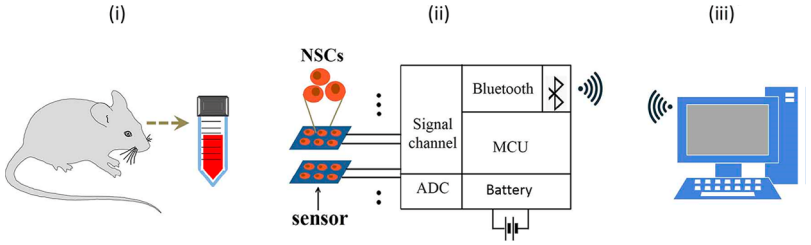

Figure 1. Schematic diagram of the cell culture on the thin-film platinum resistance sensor and the real-time temperature measurement system. (i) Extraction of neural stem cells from mouse; (ii) Neural stem cells grow on the surface of platinum resistor and are detected in real-time; (iii) Host computer interface: recording the history of temperature changes.

NSCs were inoculated on the surface of the platinum-resistor which was treated with rat-tail collagen. The real-time temperature of the cells was reflected by detecting the change in the resistance of the platinum-resistor. The temperature changes of the cells were captured by the host computer in real-time. Experimental results show that such system is capable of detecting temperatures on thousand-cell levels and maintaining cell viability during measurement process with 0.05 °C detection accuracy. At the same time, the system is in good repeatability and stability.

Thyroid hormones (THs) are major regulators of cell and mitochondrial metabolism. It can increase thermogenesis and affect the activities of almost all cells. Studies have shown that THs increase obligatory thermogenesis as a result of the stimulation of numerous metabolic pathways involved in development, remodeling, and delivery of energy to the tissues. Simultaneously, THs also play an important role in facultative thermogenesis interacting with the sympathetic nervous system (SNS).[25,26] In addition, research has shown that THs can increase mitochondrial dynamics and activate mitochondrial respiration during NSCs differentiation.[27] Therefore, we use the temperature measurement system to verify the temperature change of NSCs when stimulated by THs, which is helpful for understanding NSCs physiology.

EXPERIMENTAL SECTION

Neural Stem Cells Culture. Pregnant sprague-dawley (SD) mice (gestational age 14 days) were killed by cervical dislocation in accordance with the Guidelines for Animal Care and Use established by Medical School of Southeast University Institutional Animal Care and Use Committee. The cerebral cortex of the fetal mouse was removed one by one in a sterile environment, and the meninges were peeled off under a microscope field. The clean brain tissue was placed in a Petri dish (containing DMEM/F12 (1:1) medium) and diced.[28] It was then transferred to a 50 mL centrifuge tube (containing 0.3% trypsin) for digestion, and gently blow until there was no visible tissue block. The treated tissue was collected by centrifugation (5 min at 1000 r/min). After the supernatant was removed, a single-cell suspension that was subsequently passed through a 75 μm cell strainer to remove debris was produced. By adding the NSCs serum-free medium, the cell concentration was adjusted to be 5×10^8 cells/L. The final cell solution was put into the incubator for culture at a humidified cell culture incubator at 37 °C with 5% carbon dioxide (CO_2).[29−31]

Neural Stem Cells Cultured on the Platinum Resistor. The rat tail collagen was diluted to 0.012 mg/mL with sterile acetic acid (0.006 mol/L). The diluted solution (30 μL) was then added to the surface of the platinum resistor and placed in a clean bench to dry.[32] After disinfected the device with ethylene oxide, the cell solution (40 μL, 5×10^8 cells/L, number of cells of 20 000) was inoculated on the surface of the platinum resistor, and then placed in an incubator for following temperature detection.

After 24 h cell culture on platinum resistor, in order to observe whether the NSCs can grow on the surface of the platinum resistor, the platinum resistor was taken out and placed in the glutaraldehyde solution (concentration 2.5%, 4 °C) for 4 h. The cells were then fixed and maintained their original morphology.[33] Then, the cells were subjected to gradient dehydration using an ethanol solution. The morphology of the treated samples was observed using a scanning electron microscope (SEM, Ultra Plus, Zeiss, Germany).

Platinum Resistor Calibration and Electric Field Detection. In the range of 0−300 °C, the resistance of platinum resistor is proportional to temperature. It is approximately 1000 Ω at 0 °C and 2120 Ω at 300 °C. However, the temperature change of the cells is very weak. Thus, the platinum resistor needs to be accurately calibrated. The process is as follows:

Package the platinum resistors into a standard water tank. The temperature was mearsured by a standard thermometer (accuracy of 0.02 °C), ranging from 30 to 41 °C. The Kelvin four-wire test method is used to get the resistance of platinum resistor (accuracy is 0.01 Ω). By using ORIGIN (a data processing software), the above obtained data are processed.

In order to confirm whether there is an electric field on the sensor surface or not, an electrostatic field microscope (EFM, Dimension Icon, Bruker, Germany) was used to characterize the electric field distribution on the surface of the sensor. Different voltage (0, 0.5, and 1 V) was applied to the sensor when measurement.

Platinum Resistor Assembled with Cell Culture Plate. The final size of the platinum resistor is shown in Figure 2A(i). In order to enable the NSCs to grow on the surface of the platinum resistor, a frame was designed by 3D printing technology. The specific production process is as follows: first, the shape of the frame is designed by AutoCAD as shown in Figure 2A(ii), and then processed by Stereo lithography Appearance (SLA). As shown in Figure 2B, after placing the platinum resistor on the bottom of the frame, the frame was fixed in a cell culture plate. During the experiment, the cell solution was added into the frame, and the medium or PBS was introduced into the cell culture plate to prevent the cell solution from evaporating.

Wireless Multichannel System. In order to realize the long time cell temperature change monitoring during the cell culturing, a wireless multichannel system is designed. The

https://dx.doi.org/10.1021/acs.analchem.9b05134
Anal. Chem. 2020, 92, 3270−3275

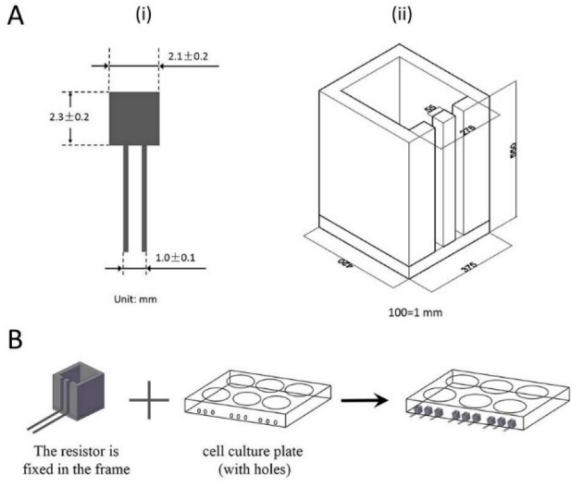

Figure 2. Size of platinum resistor and assembly process. (A) (i) The size of platinum resistor; (ii) The size of 3D printed frame. (B) Diagram of platinum resistor assembled into the culture plate.

system is mainly composed of two parts: data acquisition device and host computer system.

As shown in Figure 3A(i), the data acquisition device has 12 independent channels, and the platinum resistor is connected

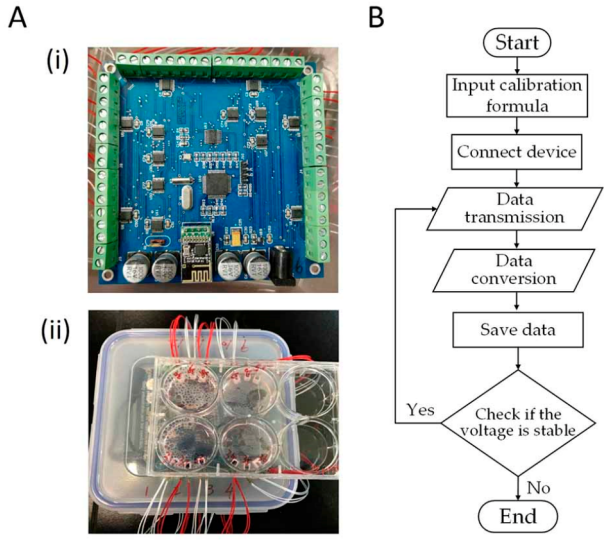

Figure 3. Hardware and software for wireless multichannel systems. (A) (i) Data acquisition device; (ii) Data acquisition device connected to thin film platinum resistor. (B) Procedure of the host computer system.

in series with the standard resistor of 1 KΩ. The acquisition device detects the voltage of the platinum resistor and the standard resistor. The resistance of platinum resistor is calculated by eq 1:

$$R_P = \frac{V_P}{V_S} \times R_S \quad (1)$$

where R_p is the resistance of platinum resistor, R_s is the resistance of standard resistor, V_P is the voltage of the platinum resistor, V_S is the voltage of the standard resistor. Finally, the data is transmitted to the host computer through Bluetooth without physical lines. The device's power comes from a lithium battery. Thus, it can be packaged and placed in an incubator as shown in Figure 3A(ii). In order to avoid the temperature change interference caused by data acquisition, the current flowing through the sensor is limited to about 0.15 mA.

The host computer system is a virtual instrument generated by LABVIEW. It is needed to input the calibration formula of each platinum resistor into the system. The working process of the system mainly includes two steps. First, the data is received through Bluetooth, then the data obtained by the different channels are processed separately. The temperature of each channel is calculated by the calibration formula of the corresponding platinum resistor. Second, the temperature data are stored in an Excel-readable file until the stop of the measurement. During the process of data storing, the system can be controlled by the software flowchart as shown in Figure 3B. Moreover, the voltage of lithium battery could be sensed. The system would be shut down when the power supply is insufficient, which ensures the accuracy of the measurement.

RESULTS AND DISCUSSION

Platinum Resistor Calibration and Electric Field Detection. The method and results of calibrating platinum resistor are shown in Supporting Information Figure S1. The temperature-resistance relationship of each platinum resistor is input into the host computer system to be calculated as the temperature of the sensor.

EFM result of the electric field of platinum resistor is shown in Figure 4A. Phase imaging mode of EFM was used in experiments. It can be seen that the value of phase is very small and does not change with the increase of the voltage. The magnitude of the phase represents the magnitude of the electrostatic force. Thus, it can be concluded that there is no electric field distributed on the sensor surface. Therefore, the voltage applied during the measurement would not affect the physiology of NSCs.

Culture and Observation of Neural Stem Cells on Platinum Resistor. First, the untreated platinum resistor was observed using SEM, which shows a flat surface with some ceramic particles, as shown in Figure 4B(i). The platinum resistor surface cultured with NSCs was then observed. The results are shown in Figure 4B(ii, iii). It demonstrates that a large number of NSCs are attached to the surface of the sensor as shown in Figure 4B(ii). The morphology of the cells was well formed, and pseudopods can be observed as shown in Figure 4B(iv). Combining the surface area of the platinum resistor with the number of cells in the SEM field of view, it was estimated that approximately 5000 cells were attached to the surface of the platinum resistor.

In order to further accurately count the number of NSCs on the surface of the sensor, the number of cells remaining in the solution was counted at 1, 2, 3, and 24 h during cell culture. The concentration of the cells was obtained by an automatic cell counter (Countess II, Invitrogen, USA). The results obtained are shown in Figure 4C and Table 1. It can be seen that the number of cells in the solution gradually decreased within 0−3 h, while the number of cells remains the same within 3−24 h. The number of cells in the solution was eventually reduced by approximately 4800, which is roughly consistent with the statistic results in the SEM characterization.

The platinum resistors without surface modification indicate no cells on the surface when SEM observation (Supporting Information Figure S2), which demonstrates that all NSCs

https://dx.doi.org/10.1021/acs.analchem.9b05134
Anal. Chem. 2020, 92, 3270−3275

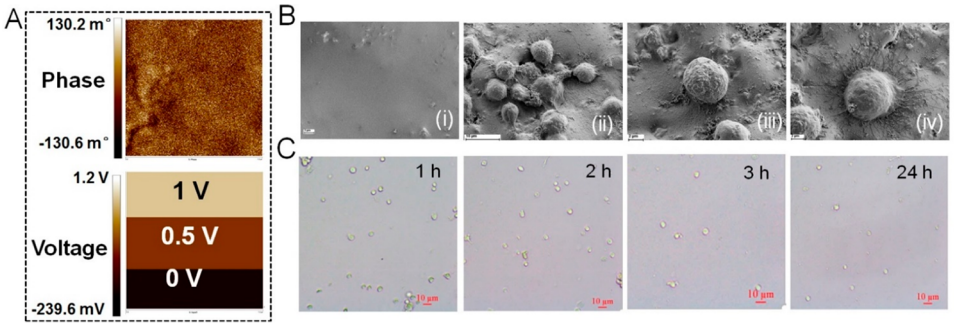

Figure 4. (A) Phase EFM characterization results with different input voltage. (B) Platinum resistor characterization under SEM after 24 h cell culture. (i) Surface topography of platinum resistance without NSCs; (ii) Cells adhere to the surface of platinum resistance; (iii) Morphology of a single cell; (iv) Pseudopods of cells. (C) Changes in cell concentration under the optical microscope, from 1 to 3 h, the concentration of cells in the solution gradually decreases. From 3 to 24 h, the cell concentration remains stable.

Table 1. Statistics of the number of cells in solution

time (h)	concentration (per mL)	cell quantity in solution	live cell ratio
1	4.63×10^5	1480	97%
2	4.16×10^5	3360	97%
3	3.81×10^5	4760	97%
24	3.79×10^5	4840	97%

grow in suspension instead of attaching to the platinum resistor surface.

Application of Multichannel System in NSCs Temperature Detection. The temperature of NSCs is detected by the above-mentioned cell culture method and the multichannel system. Three platinum resistors were placed into each well of cell culture plate with a control group (medium without NSCs) in the middle and an experimental group (medium with NSCs) on each side. The distance between control group and experimental group was less than 0.7 mm, and the temperature difference between them represents the temperature change caused by cellular activity.

As a control, the surface of some platinum resistors in the experimental group was not modified by rat tail collagen, so that all the NSCs in these groups were grown in suspension. It can be seen from Figure 5A that the temperature of the experimental group is significantly higher than that of the control group. Result in Figure 5B verifies the temperature difference between the experimental group and the control group. It can be seen that the Δt caused by the NSCs in suspension is less than 0.05 °C, almost below the temperature resolution of this system. However, the Δt caused by adherent NSCs can reach 0.35 °C. The results of repeated experiments are shown in Figure 5C. Therefore, it can be determined that Δt detected by platinum resistor is caused by adherent cells.

Furthermore, it can be seen in Figure 5B that Δt gradually increases within 0−200 min. The results in Figure 4B,C have shown that the NSCs gradually adhere to the surface of the

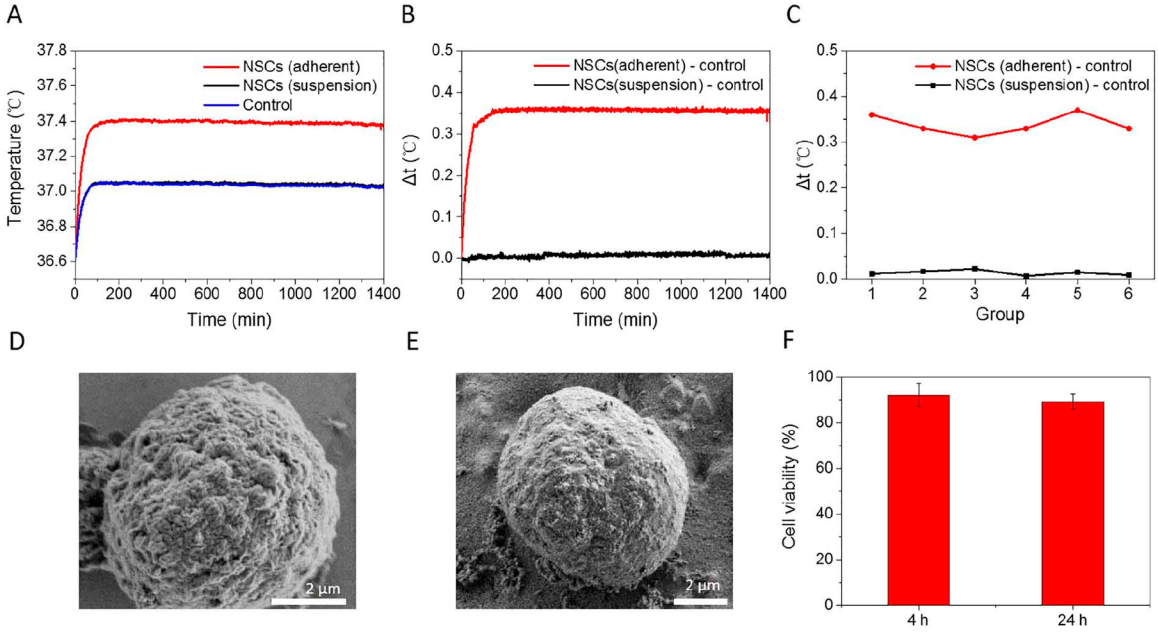

Figure 5. Temperature of NSCs. (A) Temperature of suspended NSCs and adherent NSCs. (B) Temperature difference (Δt) of suspended NSCs and adherent NSCs. (C) Temperature difference (Δt) of repeated experiments. (D) Morphology of normal NSCs under SEM (E) Morphology of NSCs after temperature detection. (F) During the temperature measurement, the viability of neural stem cells was 92% and 89% after 4 and 24 h measurement.

https://dx.doi.org/10.1021/acs.analchem.9b05134
Anal. Chem. 2020, 92, 3270−3275

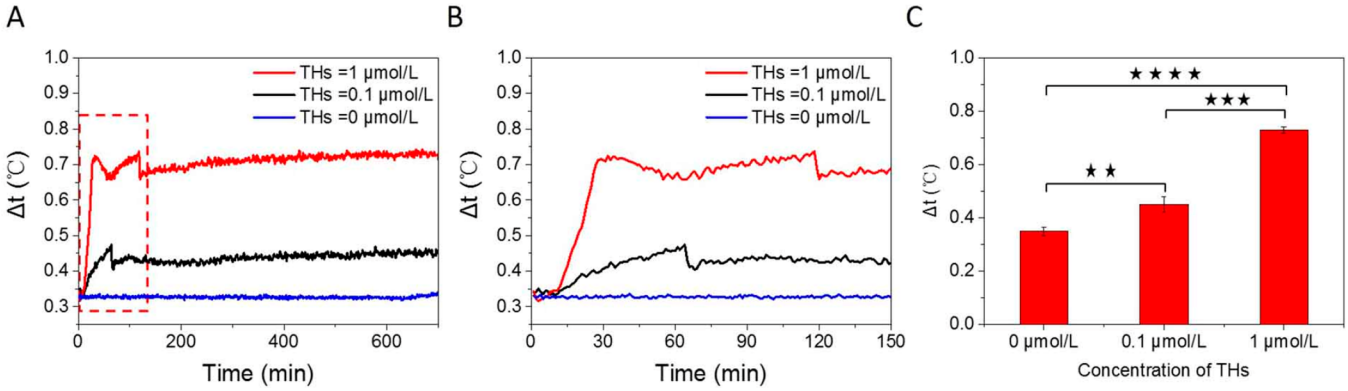

Figure 6. Effects of THs on the temperature of NSCs. (A) Changes in the temperature of NSCs stimulated by different concentrations of THs (0, 0.1, and 1 μmol/L). (B) Changes in the temperature of NSCs in the first 150 min. (C) Statistical results of temperature difference, the specific values are 0 μmol/L-0.33 °C, 0.1 μmol/L-0.45 °C, 1 μmol/L-0.72 °C.

platinum resistor from 0 to 3 h. Thus, it is also proved that the Δt detected by the sensor is caused by cell attachment.

In order to verify whether the temperature measurement method of this system affects the viability of NCSs, the morphology of normal cultured NSCs (Figure 5D) and NSCs after temperature detection (Figure 5E) were compared, both of which maintained a good cell morphology. Quantitatively, after 4 and 24 h temperature detection, CCK8 was used to detect cell viability. Result shown in Figure 5F indicates that the cell viability has been maintained above 85%, which indicates that there is no effect on cell viability when the temperature measurement changes.

Effect of Thyroid Hormone on the Temperature of Neural Stem Cells. After the NSCs are attached to the surface of the platinum resistor, the medium containing the suspended cells is taken out. Then, the medium containing different concentrations of THs (0.1, 1 μmol/L) are added to be measured. As shown in Figure 6A, the temperature started to rise after 10 min when adding THs. Compared with control group (medium without NSCs), the NSCs groups exhibit 0.45 and 0.72 °C for 0.1 and 1 μmol/L THs activation, respectively. However, the temperature of the group without THs does not change significantly. Figure 6B shows the temperature change within 150 min after the addition of THs. Compared with the group with a THs concentration of 0.1 μmol/L, the temperature of the group with a THs concentration of 1 μmol/L increased faster and the temperature was higher after stabilization. Statistical analysis shown in Figure 6C indicates that there is a significant difference between THs treated and nontreated groups. For THs treated groups, the temperature changes significantly depend on the THs concentrations.

Since the thyroid hormone may affect cell physiology through mitochondria, plasma membrane, cytoplasm and nucleus, modulation by the hormone of the basal proton leak in mitochondria accounts for a substantial component of heat production caused by THs.[34] The increase of temperature activated by THs in this study prompts that the thermogenic mechanisms of homeotherms (e.g., Na/K-ATPase, Ca^{2+} cycling) may play a key role on the heat production.[35]

CONCLUSIONS

In this study, we have developed a multichannel system for detecting the temperature of NSCs in adherent culture. Inducing NSCs to grow on the surface of the platinum resistor, the results of the SEM, and automatic cell counters showed that about 5000 cells were attached to the surface of the platinum resistor. The experimental results prove that the temperature change detected by the system is caused by the cells attached to the platinum resistance surface. The entire temperature measurement process does not affect the cell viability. In addition, thyroid hormone stimulation would significantly increase the temperature of NSCs depending on the different concentrations. This method enables noninvasive temperature detection at thousands of cell levels with multiple independent channels detection capability. Therefore, it is suitable for evaluating the thermogenic reaction of various cells and detecting metabolic changes of stem cells during proliferation and differentiation. Furthermore, it could be a reference means for detecting physiological responses of various cells under electrical, magnetic, optical, and acoustic stimulation in the future.

ASSOCIATED CONTENT

Supporting Information

The Supporting Information is available free of charge at https://pubs.acs.org/doi/10.1021/acs.analchem.9b05134.

Schematic illustration of calibrating thin-film platinum resistor, Surface of platinum resistor when NSCs grow in suspension (PDF)

AUTHOR INFORMATION

Corresponding Authors

Fang Yang − *State Key Laboratory of Bioelectronics, Jiangsu Key Laboratory for Biomaterials and Devices, School of Biological Sciences and Medical Engineering, Southeast University, Nanjing 210096, China;* orcid.org/0000-0001-6922-6348; Email: yangfang2080@seu.edu.cn

Ning Gu − *State Key Laboratory of Bioelectronics, Jiangsu Key Laboratory for Biomaterials and Devices, School of Biological Sciences and Medical Engineering, Southeast University, Nanjing 210096, China;* orcid.org/0000-0003-0047-337X; Email: guning@seu.edu.cn

Authors

Jiaxu Ding − *State Key Laboratory of Bioelectronics, Jiangsu Key Laboratory for Biomaterials and Devices, School of Biological Sciences and Medical Engineering, Southeast University, Nanjing 210096, China*

Jing Li − *State Key Laboratory of Bioelectronics, Jiangsu Key Laboratory for Biomaterials and Devices, School of Biological*

https://dx.doi.org/10.1021/acs.analchem.9b05134
Anal. Chem. 2020, 92, 3270−3275

Sciences and Medical Engineering, Southeast University, Nanjing 210096, China

Complete contact information is available at: https://pubs.acs.org/10.1021/acs.analchem.9b05134

Author Contributions

The manuscript was written by J.D. and F.Y. through contributions of all authors. F.Y. and N.G. contributed to the initial concept and supervised the work. J.D. and F.Y. conceived the overall experimental strategy. J.D. perfomed the whole experiments. J.L. helped to culture the cells and SEM characterization.

Notes

The authors declare no competing financial interest.

■ ACKNOWLEDGMENTS

This investigation was financially funded by the National Key Research and Development Program of China (2017YFA0104302, 2018YFA0704103) and the National Natural Science Foundation of China (81971750). Funding also partially comes from the Natural Science Foundation of Jiangsu Province (BK20191266), Six Talent Peaks Project of Jiangsu Province (2017-SWYY-006), and Zhong Ying Young Scholar of Southeast University. We also thank the support from the Fundamental Research Funds for the Central Universities.

■ ABBREVIATIONS

NSCs	neural stem cells
SEM	scanning electron microscopy
ATP	adenosine-triphosphate
ESC	embryonic stem cells
AFM	atomic force microscope
SD	Sprague−Dawley
CO_2	carbon dioxide
SLA	stereo lithography appearance
THs	thyroid hormones

■ REFERENCES

(1) Temple, S. *Nature* **2001**, *414*, 112−117.
(2) Tornero, D.; Tsupykov, O.; Granmo, M.; Rodriguez, C.; Gronning-Hansen, M.; Thelin, J.; Smozhanik, E.; Laterza, C.; Wattananit, S.; Ge, R. M.; Tatarishvili, J.; Grealish, S.; Brustle, O.; Skibo, G.; Parmar, M.; Schouenborg, J.; Lindvall, O.; Kokaia, Z. *Brain* **2017**, *140*, 692−706.
(3) Amemori, T.; Romanyuk, N.; Jendelova, P.; Herynek, V.; Turnovcova, K.; Prochazka, P.; Kapcalova, M.; Cocks, G.; Price, J.; Sykova, E. *Stem Cell Res. Ther.* **2013**, *4*, 15.
(4) Akhavan, O.; Ghaderi, E. *Nanoscale* **2013**, *5* (21), 10316−10326.
(5) Wang, Z.; Wang, Y.; Wang, Z. Y.; Zhao, J.; Gutkind, J. S.; Srivatsan, A.; Zhang, G. F.; Liao, H. S.; Fu, X.; Jin, A.; Tong, X.; Niu, G.; Chen, X. Y. *ACS Nano* **2015**, *9*, 6683−6695.
(6) Bond, A. M.; Ming, G. L.; Song, H. J. *Cell Stem Cell* **2015**, *17*, 385−395.
(7) Bernstock, J. D.; Peruzzotti-Jametti, L.; Ye, D.; Gessler, F. A.; Maric, D.; Vicario, N.; Lee, Y. J.; Pluchino, S.; Hallenbeck, J. M. *J. Cereb. Blood Flow Metab.* **2017**, *37*, 2314−2319.
(8) Homem, C. C. F.; Repic, M.; Knoblich, J. A. *Nat. Rev. Neurosci.* **2015**, *16*, 647−659.
(9) Conti, L.; Cattaneo, E. *Nat. Rev. Neurosci.* **2010**, *11*, 176−187.
(10) Folmes, C. D. L.; Nelson, T. J.; Martinez-Fernandez, A.; Arrell, D. K.; Lindor, J. Z.; Dzeja, P. P.; Ikeda, Y.; Perez-Terzic, C.; Terzic, A. *Cell Metab.* **2011**, *14*, 264−271.
(11) Goncalves, J. T.; Schafer, S. T.; Gage, F. H. *Cell* **2016**, *167*, 897−914.
(12) Zhang, H.; Badur, M. G.; Divakaruni, A. S.; Parker, S. J.; Jager, C.; Hiller, K.; Murphy, A. N.; Metallo, C. M. *Cell Rep.* **2016**, *16*, 1536−1547.
(13) Zhang, X. D.; Boyer, L.; Jin, M. J.; Mertens, J.; Kim, Y. S.; Ma, L.; Ma, L.; Hamm, M.; Gage, F. H.; Hunter, T. *eLife* **2016**, *5*, 25.
(14) Ito, K.; Suda, T. *Nat. Rev. Mol. Cell Biol.* **2014**, *15* (4), 243−256.
(15) Akhavan, O.; Ghaderi, E.; Shirazian, S. A. *Colloids Surf., B* **2015**, *126*, 313−321.
(16) Akhavan, O.; Ghaderi, E.; Aghayee, S.; Fereydooni, Y.; Talebi, A. *J. Mater. Chem.* **2012**, *22*, 13773−13781.
(17) Wang, C. L.; Xu, R. Z.; Tian, W. J.; Jiang, X. L.; Cui, Z. Y.; Wang, M.; Sun, H. M.; Fang, K.; Gu, N. *Cell Res.* **2011**, *21*, 1517−1519.
(18) Li, C.; Sun, J. F.; Wang, Q. W.; Zhang, W. G.; Gu, N. *IEEE Trans. Biomed. Eng.* **2019**, *66*, 23−29.
(19) Vetrone, F.; Naccache, R.; Zamarron, A.; de la Fuente, A. J.; Sanz-Rodriguez, F.; Maestro, L. M.; Rodriguez, E. M.; Jaque, D.; Sole, J. G.; Capobianco, J. A. *ACS Nano* **2010**, *4*, 3254−3258.
(20) Tanimoto, R.; Hiraiwa, T.; Nakai, Y.; Shindo, Y.; Oka, K.; Hiroi, N.; Funahashi, A. *Sci. Rep.* **2016**, *6*, 10.
(21) Yang, J. M.; Yang, H.; Lin, L. W. *ACS Nano* **2011**, *5*, 5067−5071.
(22) Majumdar, A. *Annu. Rev. Mater. Sci.* **1999**, *29*, 505−585.
(23) Li, C.; Yan, S.; He, W. N.; Yang, S.; Sun, J. F.; Gu, N. *IEEE Trans. Biomed. Eng.* **2019**, *66*, 1898−1904.
(24) Bai, T. T.; Gu, N. *Small* **2016**, *12*, 4590−4610.
(25) Yen, P. M. *Physiol. Rev.* **2001**, *81*, 1097−1142.
(26) Silva, J. E. *Thyroid* **1995**, *5*, 481−492.
(27) Gothie, J. D.; Sebillot, A.; Luongo, C.; Legendre, M.; Van, C. N.; Le Blay, K.; Perret-Jeanneret, M.; Remaud, S.; Demeneix, B. A. *Mol. Metab.* **2017**, *6*, 1551−1561.
(28) Song, S. H.; Stevens, C. F.; Gage, F. H. *Nature* **2002**, *417*, 39−44.
(29) Kopach, O.; Rybachuk, O.; Krotov, V.; Kyryk, V.; Voitenko, N.; Pivneva, T. *J. Cell Sci.* **2018**, *131*, 10.
(30) Saha, K.; Keung, A. J.; Irwin, E. F.; Li, Y.; Little, L.; Schaffer, D. V.; Healy, K. E. *Biophys. J.* **2008**, *95*, 4426−4438.
(31) Rietze, R. L.; Valcanis, H.; Brooker, G. F.; Thomas, T.; Voss, A. K.; Bartlett, P. F. *Nature* **2001**, *412*, 736−739.
(32) Ma, F. K.; Zhu, T. M.; Xu, F.; Wang, Z. F.; Zheng, Y. T.; Tang, Q. S.; Chen, L. P.; Shen, Y. W.; Zhu, J. H. *Acta Biomater.* **2017**, *50*, 188−197.
(33) Jiang, P.; Chen, C.; Wang, R. M.; Chechneva, O. V.; Chung, S. H.; Rao, M. S.; Pleasure, D. E.; Liu, Y.; Zhang, Q. G.; Deng, W. B. *Nat. Commun.* **2013**, *4*, 16.
(34) Cheng, S. Y.; Leonard, J. L.; Davis, P. J. *Endocr. Rev.* **2010**, *31*, 139−170.
(35) Danzi, S.; Klein, I. *Med. Clin. North Am.* **2012**, *96*, 257−268.